Methods

Florian Pfaff*, Christoph Pieper, Georg Maier, Benjamin Noack, Robin Gruna, Harald Kruggel-Emden, Uwe D. Hanebeck, Siegmar Wirtz, Viktor Scherer, Thomas Längle and Jürgen Beyerer

Predictive tracking with improved motion models for optical belt sorting

Prädiktives Tracking mit verbesserten Bewegungsmodellen für die optische Schüttgutsortierung

Abstract: Optical belt sorters are a versatile means to sort bulk materials. In previous work, we presented a novel design of an optical belt sorter, which includes an area scan camera instead of a line scan camera. Line scan cameras, which are well-established in optical belt sorting, only allow for a single observation of each particle. Using multitarget tracking, the data of the area scan camera can be used to derive a part of the trajectory of each particle. The knowledge of the trajectories can be used to generate accurate predictions as to when and where each particle passes the separation mechanism. Accurate predictions are key to achieve high quality sorting results. The accuracy of the trajectories and the predictions heavily depends on the motion model used. In an evaluation based on a simulation that provides us with ground truth trajectories, we previously identified a bias in the temporal component of the prediction. In this paper, we analyze the simulation-based ground truth data of the motion of different bulk materials and derive models specifically tailored to the generation of accurate predictions for particles traveling on a conveyor belt. The derived models are evaluated using simulation data involving three different bulk materials.

*Corresponding author: Florian Pfaff, Intelligent Sensor-Actuator-Systems Laboratory (ISAS), Karlsruhe Institute of Technology (KIT), Karlsruhe, Germany, e-mail: florian.pfaff@kit.edu
Christoph Pieper, Siegmar Wirtz, Viktor Scherer, Department of Energy Plant Technology (LEAT), Ruhr-Universität Bochum (RUB), Bochum, Germany
Georg Maier, Robin Gruna, Thomas Längle, Jürgen Beyerer, Fraunhofer IOSB, Fraunhofer Institute of Optronics, System Technologies and Image Exploitation, Karlsruhe, Germany
Benjamin Noack, Uwe D. Hanebeck, Intelligent Sensor-Actuator-Systems Laboratory (ISAS), Karlsruhe Institute of Technology (KIT), Karlsruhe, Germany
Harald Kruggel-Emden, Mechanical Process Engineering and Solids Processing (MVTA), Technical University Berlin, Berlin, Germany

The evaluation shows that the constant velocity model and constant acceleration model can be outperformed by utilizing the similarities in the motion behavior of particles of the same type.

Zusammenfassung: Optische Bandsortierer sind vielseitige Maschinen zur Sortierung von Schüttgütern. In vorangegangenen Arbeiten haben wir ein neues Design eines optischen Bandsortierers vorgeschlagen, in dem eine Flächenkamera anstelle einer Zeilenkamera eingesetzt wird. Zeilenkameras, die in optischen Bandsortierern etabliert sind, erlauben nur eine einmalige Beobachtung eines jeden Partikels. Mithilfe von Multitarget-Tracking-Verfahren können die Daten der Flächenkamera dazu verwendet werden, einen Teil der Trajektorien der Teilchen zu bestimmen. Das Wissen über die Trajektorien kann genutzt werden, um vorherzusagen, wann und wo die Teilchen an dem Separationsmechanismus vorbeifliegen. Akkurate Vorhersagen sind essenziell, um hochqualitative Sortierergebnisse zu erzielen. Die Genauigkeit der Trajektorien und Vorhersagen hängt stark von dem eingesetzten Bewegungsmodell ab. In einer Evaluation basierend auf einer Simulation, welche die wahren Trajektorien liefert, wurde zuvor ein Bias in den Vorhersagen identifiziert. Im vorliegenden Beitrag analysieren wir die Trajektorien unterschiedlicher Schüttgüter in Simulationen und leiten Bewegungsmodelle her, die auf die Vorhersage der Bewegung von Schüttgutteilchen auf einem Förderband zurechtgeschnitten sind. Die vorgestellten Modelle werden anhand Simulationen dreier Schüttgüter evaluiert. In der Evaluation zeig sich, dass Modelle, die Ähnlichkeiten im Bewegungsverhalten gleichartiger Teilchen berücksichtigen, die Constant-Velocity- und Constant-Acceleration-Modelle in ihrer Vorhersagegenauigkeit übertreffen können.
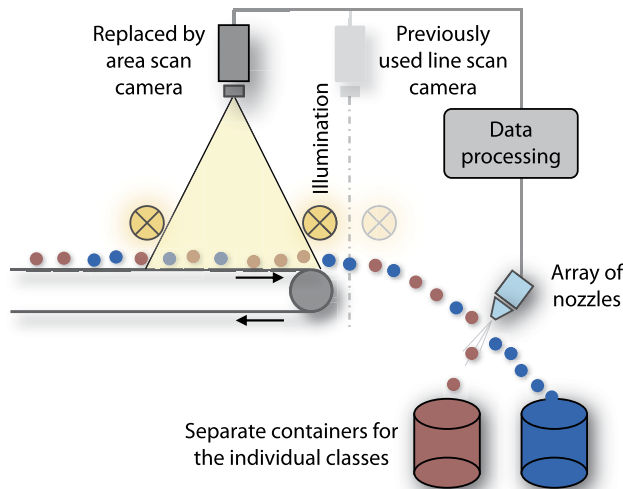
Figure 1: Schematic view of an optical belt sorter. Industrial optical belt sorters use a line scan camera to observe the particles. An area scan camera is used in the approach proposed in [8].

Schlagwörter: Bewegungsmodelle, Multitarget Tracking, optische Sortierung

1 Introduction

Current technological advances result in an increase in automation, both because new tasks can be handled by machines and because the machines employed are improving, reducing the necessity of human labor in the respective task. Very important industrial processes are the processing, shipping, and handling of bulk material, which are estimated to consume about 10% of all energy produced worldwide [1]. For separating or purifying bulk materials such as ores, industrial minerals, and recycling materials (including plastics, glass, and metals), classical methods are density [2] and magnetic separation [3]. In the recent years, sensor-based sorters, which make use of algorithmic innovations and the declining cost of computation power, have become an important means to sort bulk material. While sensor-based sorters were (compared with, e. g., magnetic separations) only recently developed, they are already established for mineral sorting [4], recycling [5], and removing contaminants from food products [6, Ch. 5]. However, they are complex machines, both mechanically and in terms of data processing, and they have many degrees of freedom that can be used to improve the sorter design.

In this paper, we focus on optical belt sorters, as illustrated in Fig. 1, that use air jets to separate the stream of bulk material. The bulk material is first applied to a conveyor belt. On this belt, the particles of the bulk material are assumed to attain a specific velocity along the transport direction and come to a halt along the direction orthogonal to it. The particles start an approximately parabolic flight path when leaving the belt. Each particle is localized and classified using an imaging sensor, e. g., a line scan camera. Thereafter, the particles pass an array of nozzles that is aligned orthogonally to the transport direction. Depending on the classification result, one (or multiple) valves are activated to emit air jets from specific nozzles. Particles that are hit by air jets do not follow the same flight parabola as particles that are not hit. Thus, the particles are divided into two fractions. The two fractions can, e. g., land in different containers (as illustrated in Fig. 1) or on different chutes or slides that transport them to the next processing steps. Sensor-based sorters are often employed to clean a stream of bulk material from contaminants or to extract valuable products from a stream consisting mostly of waste. In such applications, one of the fractions is supposed to consist only of valuable particles, whereas the other fraction should consist only of waste. How severe it is when waste particles land in the fraction of valuable particles or when valuable particles land in the waste fraction strongly depends on the application.

Currently employed industrial optical belt sorters are equipped with one or multiple [7] line scan cameras that observe particles of the bulk material passing their field of view. Central to this approach is the assumption that all particles attain a well-known velocity. First, the assumption is used to obtain a two-dimensional RGB image of the particles, and deviations from the assumed velocity can cause color fringes or distortions of the particles' shapes. Second, as described in detail later in this paper, the assumed velocity is used to generate predictions of the particles' motions after the localization based on the line scan camera image. Due to delays in the data processing and control of the valves, there is a time frame of about 20–40 ms between the observation and the separation. During this time, the decision if any valve should be activated (and if so, how many and which ones) needs to be made. The simple, currently established policy is to trigger one or multiple valves at a fixed time after the observation. For line scan camera-based sorters, the choice of the valve to activate is based on an assumed straight flight path along the transport direction.

If the contours of the bulk material particles can be recognized in area scan camera images of the bulk material stream (which may be challenging for high loads), an approach based on area scan cameras can be employed [8]. Using this approach, improved predictions can

be generated, which in turn can be used to enhance the separation process. As the particles are tracked to increase the accuracy of the predictions to bridge the temporal gap, we refer to this approach as predictive tracking. The use of the predictive tracking approach comes with many opportunities, such as improving the classification [9], but also gives rise to a variety of challenges.

Predictive tracking comprises two essential building blocks. First, a real-time capable multitarget tracking algorithm [10, 11], as presented in [12, 13], is used to track the particles. Second, a prediction is performed in each time step as to when and where each particle will pass the separation mechanism. If, according to the prediction, there will be too little time remaining to also incorporate the data of the next time step, a policy to determine which valve should be activated is employed. To achieve a reliable decision as to which valve to activate and when to activate it, we require an accurate prediction, which itself requires an accurate model of the particles' motions.

Further, accurate motion models are important for the tracker. One of the key challenges in multitarget tracking arises when it is unknown which actual object a measurement stems from. This problem arises in bulk material sorting tasks as distinguishing all particles on the belt based on visual features is either impossible or computationally too demanding. As described in [8], we use a global nearest neighbor (GNN) [10, Sec. 6.4] as the multitarget tracker and integrate information about the scenario at hand, such as where particles tend to enter and exit the observable area. The GNN associates each measurement with (at most) one of the already known particles. The reliability of the association between the known particles and measurements and the assessment whether a particle is observed for the first time or has left the belt is key to the success of the approach. Both can be improved significantly by increasing the accuracy of the predictions of the known particles' motions.

In our project, we have created and modeled a laboratory-scale optical belt sorter that serves as an experimental platform to improve the design of optical belt sorters and enhance the algorithms employed. Using accurate simulations of this sorter [14] not only allows us to optimize the sorter design but also to evaluate the predictive tracking approach. In [15], we tested the accuracy of the derived predictions using simulation data. Due to the availability of all positions at a very high sampling rate, we have accurate reference values to evaluate the predictions against. In [15], we closely regarded a tracker based on a simple motion model and identified a major shortcoming of the model. In the current paper, we regard simulations

of three different bulk materials and present motion models tailored to the bulk material sorting task. The models were first described in [16, Ch. 4].

The paper is structured as follows. In the second section, we provide a brief explanation of and motivation for the predictive tracking approach. In the third section, we provide some details on the simulations and the sorter they are based on. The novel models are described in the fourth section. An evaluation of various models is presented in the fifth section. In the last section, we provide a conclusion and an outlook.

2 Predictive tracking for optical belt sorters

The motivation for predictive tracking comes from the deficiencies of the simple model as used in systems based on line scan cameras. Unless extensions that make use of the different color channels (as laid out in [17]) are employed, only one observation of each particle is obtained. Using only one observation makes strong assumptions about each particle's movement a necessity. Without information on the movement orthogonal to the transport direction, the assumption of a straight movement is usually the best. The temporal offset between the observation by the line scan camera and the arrival at the separation mechanism is often determined experimentally. If we assume that the distribution of the velocities is symmetrical and that predicting a point in time that is too early has an identical impact on the sorting performance as predicting a point in time that is too late, the average delay for previously observed particles can be used to maximize the hit ratio under the given assumptions. As the average delay is often respected in the sorter design without explicitly specifying a motion model, we refer to this model as the old, implicit model.

In practical applications, the alignment of the belt, camera, and array of nozzles is never truly perfect. The temporal calibration is also prone to errors as it is determined experimentally and changes in the particles' motion behavior are possible due to, e. g., dirt accumulating on the belt. Even if the temporal and spatial calibration were perfect, there may be a lot of variation in the motion behavior of the particles. The actual deviations from the assumed flight paths depend on both the sorter design and the bulk material sorting task at hand. Costly or inconvenient extensions, such as using a longer belt or using fluted surfaces that are harder to clean, are used to further adapt the particles' motions to the expected behavior.
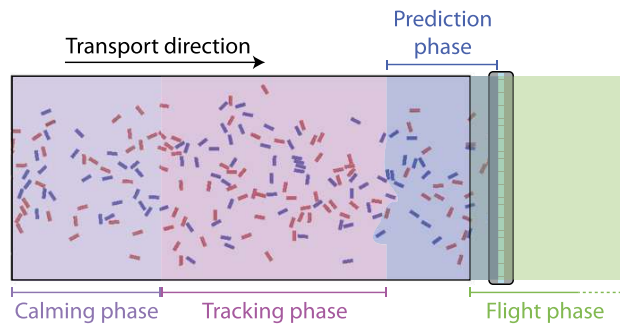
Figure 2: Visualization of the different phases. All particles shown are cylinders and the colors of the particles indicate whether they should be separated from the bulk material stream. Whether a particle is in the prediction phase depends not only on the particle's position but also its velocity. The depiction of the tracking and prediction phases as regions is only intended to illustrate the concepts, and the actual boundaries may change in every time step. Adapted version of an illustration from [16].

However, these adaptations have their limits and a considerable variation in the velocities is almost impossible to eliminate. Both the variation in the flight directions of the particles and possible calibration errors can be observed in the evaluation based on real data in [8].
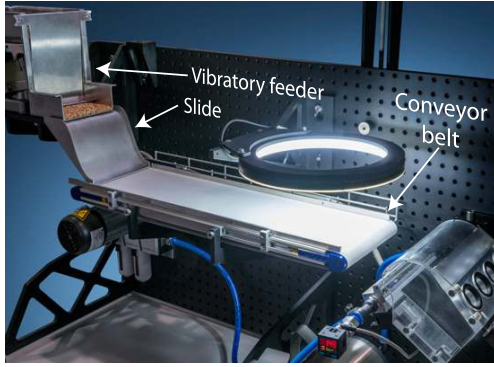
To reduce assumptions about the motion behavior of the particles, we proposed to observe the particles over multiple time steps using an area scan camera [8]. We begin by tracking all particles in a tracking phase, as shown in Fig. 2. Based on the trajectories derived during the tracking phase, we predict how the particles will move in the prediction phase.[1] As long as no errors are made when determining which measurements stem from the same particle, imprecisions in the models can be tolerated in the tracking phase because measurements are obtained at regular time intervals. Measurements obtained during the prediction phase cannot be used, and thus, the accuracy of the motion models is crucial for obtaining highly accurate predictions to the separation mechanism.

A very accurate model for the prediction of the particles' motions can be derived by building upon the laws of physics. In the next section, we outline such a model, which we used to simulate sorting scenarios. However, this model is complicated and requires the accurate characteristics of the bulk material. These are usually not available in real-world applications—particularly when the valuable particles and waste comprise different types of particles
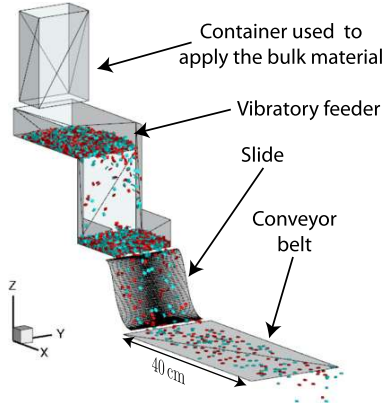
that are hard to distinguish visually or when contaminants are unknown ahead of time. Further, at the current state of the art of numerical simulation, it would be impossible to achieve the required run times. To keep the prediction phase short and achieve high frame rates (which increase the reliability of the tracker), very low run times are important. Besides being too slow, current numerical simulation algorithms do not account for uncertainties, which are required for the multitarget tracking algorithm. Therefore, we resort to models that do not need in-depth information about the particles. To be able to use a simple tracker and ensure its real-time performance, we limit ourselves to motion models that can be written as linear functions in discrete time.

In [15], we used a constant velocity (CV) model [18, Sec. III] that is based on the assumption that the velocity of each particle stays approximately constant. This model allows for reliable associations between the tracks and the measurements and is thus sufficiently accurate to successfully track the particles while they are in the tracking phase. To assess the overall performance of the predictive tracking approach with a constant velocity model, we performed multiple evaluations. Using real image data recorded on an industrial-scale optical belt sorter, we showed that the predictions as to where the particles will pass the array of nozzles are significantly better when using a constant velocity model than when using the old, implicit model assuming movement straight in the transport direction [8]. For further studies, a small experimental (but fully functional) optical belt sorter called TableSort was created. The computer-aided design (CAD) model that was created to build the sorter was also used for the simulations [14, 19], which are based on the discrete element method (DEM) [20]. Among other properties of the optical belt sorter, the hit ratio and ratio of co-deflections for the old, implicit model and the constant velocity model were analyzed using numerical simulations in [14]. To ensure optimal conditions, the positions and velocities were directly obtained from the simulation and not estimated using tracking. Using simplified assumptions about the separation mechanism, the quality of the separation result is given for several configurations of parameters such as the number of valves, the length of the prediction phase, the duration of the valve activation, and the particle mass. In [21], the multitarget tracking algorithm from [8] was used based on the position data of the simulation to derive the velocities and thus also the predictions. Furthermore, the separation using air jets was implemented using computational fluid dynamics to include all aspects of the real sorter in the simulation.

---

1 The prediction phase is not only present when using predictive tracking, but also when using the old, implicit model. For sorters using line scan cameras, the prediction phase is usually part of the flight phase.

(a) Photo of TableSort.

(b) Three-dimensional model of TableSort as used in the DEM.

Figure 3: Photo of the TableSort system and corresponding 3-D model.

3 Experimental platform and simulation methodology

Our experimental platform TableSort, shown in Fig. 3a, allows for easily changing hardware components to swiftly make adaptions to the sorter. TableSort includes all components of a common industrial-scale optical belt sorter, and all components can be attached at varying locations to a rear panel, which is similar to an optical breadboard. We used this sorter in our simulations as adaptions to the simulation can be easily realized in the real sorter and

vice versa, which allows us to validate the simulation and match the real sorter to the simulation. In the configuration modeled for our current paper, TableSort is equipped with a belt of 40 cm length and 18 cm width.

The key to evaluating the motion models of the tracker is an accurate numerical simulation with high temporal and spatial resolution. Unlike in evaluations based on real image data, the availability of a ground truth allows us to reliably assess the accuracy of the predictions. The DEM simulations are based on Newton's and Euler's equations of motion and respect both the interaction of particles with the components of the sorter and with each other. After determining the vector-valued contact force $\underline{F}_i^c$, the acceleration of the ith particle's centroid $\underline{p}_i$ can be described using

$$m_i \frac{d^2 \underline{p}_i}{dt^2} = \underline{F}_i^c + \underline{F}_i^g \,,$$

depending on the mass m_i of the ith particle and the gravitational force $\underline{F}_i^g$. In the evaluation in our current paper, we assess the accuracy of the predicted time and place at which the separation mechanism is reached. For this, the separation process, which is considered in [22, 21], does not need to be modeled. For the angular acceleration $\frac{dW_i}{dt}$, the equation for the ith particle is

$$\mathbf{I}_i \frac{dW_i}{dt} + \underline{W}_i \times (\mathbf{I}_i \underline{W}_i) = \mathbf{\Lambda}_i^{-1} \underline{M}_i \,,$$

depending on the inertia tensor along the principal axis $\mathbf{I}_i$, the angular velocity $\underline{W}_i$, and the rotation matrix $\mathbf{\Lambda}_i^{-1}$ converting the contact force vector $\underline{M}_i$ from the inertial frame to the body-fixed frame. We refer the reader to [14, 23] for more details on our simulation and the DEM.

The DEM requires knowledge about the physical properties of the individual parts of the sorter and of the particles of the bulk materials. These parameters were determined experimentally based on the approach in [24]. The ground truth data used in this paper were generated using a DEM simulation with a time step of 0.1 ms, which corresponds to a sampling rate of 10 000 Hz.

4 Improved models

Motion models are required in two parts of the predictive tracking approach. First, a motion model is used to propagate the current knowledge about the particles to the next time step. This allows us to accurately fuse information over multiple time steps in the tracking phase. Second, motion models are important for the prediction to the separation mechanism, which is used to bridge the prediction

Further studies on the accuracy of the predictions obtained using the constant velocity model were performed based on simulation data in [15]. Most importantly, we identified a bias in the temporal component of the predictions. In our current paper, we address this bias and describe models that are tailored to the bulk material sorting application.

phase. Different models can be used for the two predictions.

In this paper, we focus on the prediction to the separation mechanism. Due to the longer prediction horizon, this is the more challenging task. Adapted models for the prediction to the next time step could also be derived based on the ideas presented in this section. For such models, formulae to update the covariance matrices would also be required. In our experience, reliable associations can even be obtained using a CV or constant acceleration (CA) [18] model for the prediction to the next time step when the frame rate is sufficiently high.

A central aim of our novel models for the prediction to the separation mechanism is to eliminate the bias that we observed in our evaluation of the predictions of the CV model in [15]. The observed bias indicates that the particles arrive earlier than anticipated. By analyzing the velocities of the particles, we deduced that the bias is caused by an ongoing acceleration of the particles during the prediction phase. Since the flight phase should be as short as possible to reduce the spread in the flight paths of the particles, we predict the particles' positions at the end of the belt and assume that the separation occurs immediately when the particles enter the flight phase.[2] Hence, the prediction phase in [15] and our current paper is entirely on the belt. Since the particles are significantly slower than the belt when entering the prediction phase, the particles accelerate during the prediction phase.

To find suitable models, we first analyzed the velocities and accelerations of the particles in the ground truth data. To simplify the explanations, we call the axis along the transport direction *x*-axis and the axis orthogonal to the transport direction *y*-axis. The belt thus has an extent of 40 cm along the *x*-axis and 18 cm along the *y*-axis. In the following paragraphs, we start by describing the scenarios considered. Afterward, we go into detail on the essential components of a separation decision, and then, we explain how additional parameters for the new models can be derived.

Scenarios

In each of our three simulations, we regard a different bulk material as we expect the performance of the models to be highly dependent on the bulk material considered. First,

(a) Example of a valve activation decision.

(b) Example in which the wrong valve is chosen.

(c) Example in which the valve is activated at the wrong time.

Figure 4: Illustration of valve activation decisions for a small array of 8 nozzles with 8 corresponding valves. The optimal decision is shown in green and bad decisions based on inaccurate predictions are shown in red.

the spheres regarded in [15] were simulated using a different friction coefficient between the particles and the belt. The spheres are modeled after wooden spheres with a radius of 2.5 mm. Second, wooden cylinders with a height of 9 mm and a radius of 1.5 mm were considered. The third bulk material consisted of wooden cuboids with edge lengths of 2 mm, 5 mm, and 6 mm. In each simulation, approximately 0.2 kg of each bulk material was applied, which corresponds to 3713 spheres, 4427 cylinders, and 4357 cuboids. In all scenarios, TableSort was used as the optical belt sorter. The belt in the simulation runs at a velocity of 1.5 m/s. In the development of the new models, we use the ground truth data downsampled to 1000 Hz.

Components of the separation decision

As illustrated in Fig. 4a, there are multiple degrees of freedom in the valve activation decisions. First, the valve (or valves) to activate must be chosen. The prediction of the position along the *y*-axis is used for this decision. An inaccurate prediction for this axis can lead to an activation of an incorrect valve (see Fig. 4b). Second, the time at which the valve should be activated needs to be set. To determine a suitable time, an accurate prediction when the particle will arrive at a certain coordinate along the *x*-axis is crucial. As sketched in Fig. 4c, an inaccurate prediction can lead to a valve activation decision that may not ensure the successful ejection of the particle. A possible third parameter is the duration of the valve activation. In practical applications, the duration depends on the shape of the particles and the accuracy of the predictions. The duration is

---

2 In practice, a small overlap of the prediction phase and flight phase is inevitable. However, the flight phase can be kept much shorter than in commonly-used line scan camera-based sorters that only observe the particles when they are already in flight. For these, the entire prediction phase is a part of the flight phase.
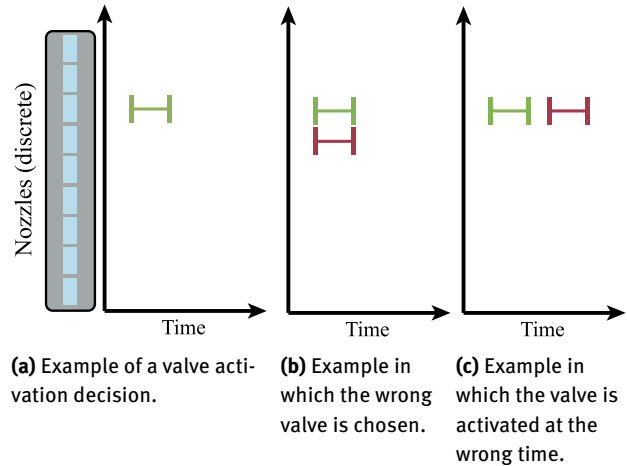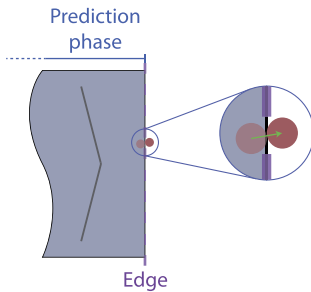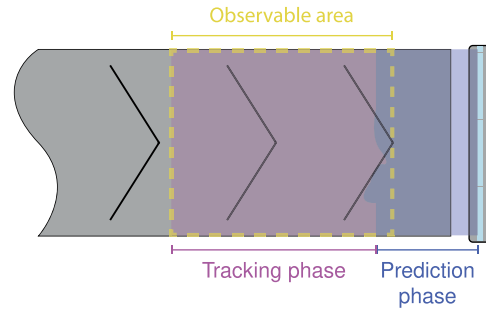
Figure 5: Approach to obtain reference values for the intersection. The motion is linearly interpolated between the last observation before (shown semiopaque) and the first observation (completely opaque) after the edge. Adapted version of an illustration from [16].

(a) Configuration in which the prediction phase is not observed.

(b) Configuration in which the prediction phase is observed. The tracking phase becomes smaller as it limited to the observable area.

Figure 6: Possible observable areas for the predictive tracking approach (assuming the array of nozzles is placed below the flight parabola).

increased when the predictions are known to be inaccurate to ensure that the particles will be hit nonetheless. However, this comes at the cost of a higher consumption of compressed air and an increased ratio of particles that are inadvertently hit (so-called co-deflections). In this paper, we do not consider the activation duration of the valves. However, it can be safely assumed that the particles can be hit reliably with a shorter activation duration if the temporal predictions of the centroids are more accurate.
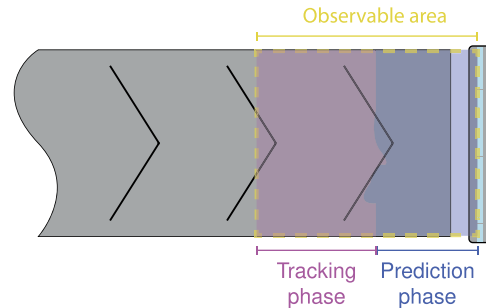
Approximating additional parameters

For some models, we need to approximate parameters such as the average time t^{Avg} between the last observation of a particle and its arrival at the separation mechanism. To derive such parameters from the simulation data, we first determine reference values for the intersection with the line to which we predict (in this paper, the edge of the belt) for each particle, as illustrated in Fig. 5. The y-coordinate of the intersection is the point at which the linearly interpolated trajectory of the particle passes the edge. To obtain the accurate point in time at which the particle had crossed the edge, we regarded the position at the last time step before the intersection and the position at the first time step thereafter. Then, we calculated the distance between these two positions. Further, we determined the distance between the actual intersection and the position of the particle at the last time step before the intersection. The ratio between these two distances was used to determine the accurate point in time of the intersection with sub-millisecond precision. By doing so, we essentially assume that the particle has a constant velocity between these two points. However, since we interpolated the motion only for a tenth of a millisecond, the determined point in time can safely be considered accurate.

Depending on the placement of the camera, the required observation before and after the line to which we predict may be unavailable in real-world scenarios. To obtain these observations, the observable area can be changed, as sketched in Fig. 6. This change allows for tracking the particles even after the separation decision was performed. Changing the observable area results in fewer measurements that can be used to predict the particles' motions during the prediction phase. However, as long as a sufficient number of measurements is obtained during the tracking phase, the tracking accuracy does not decrease significantly. To obtain the observations before and after the line at which the separation is supposed to occur, it may be necessary to disable the separation mechanism in a dedicated calibration phase, which is solely used to obtain the required parameters of the model. The setup shown in Fig. 6b is then only required in the calibration phase, while the setup in Fig. 6a can be used for tracking when the sorter is switched to sorting mode. As will become evident in our explanation of the models, a calibration phase, usually in the form of experiments, is also required for the old, implicit model.

In the following subsections, we regard the two axes separately as the effects of the belt may lead to different motion behaviors along the two axes. The old, implicit model is also subdivided into the parts along and orthog-
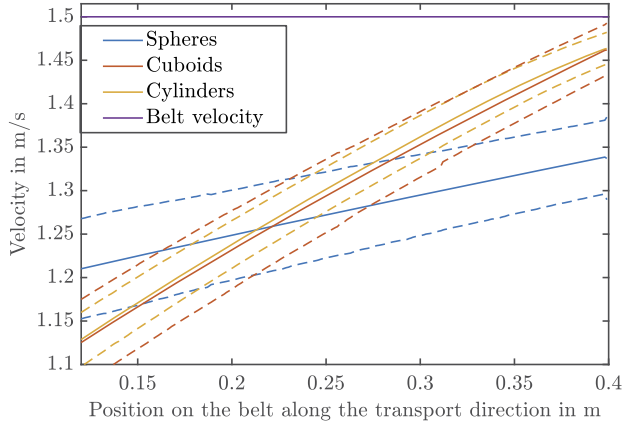
Figure 7: Mean velocities and standard deviations plotted over a part of the belt for all data sets. The dotted lines indicate $\pm 1\sigma$ added to the mean. The belt velocity is also shown for reference. Adapted version of an illustration from [16].

onal to the transport direction to emphasize the different assumptions. For all models considered, it is possible to first derive the time remaining until the separation mechanism is reached and then calculate the spatial prediction based on the remaining time and additional information. Therefore, we can consider different combinations of models for the motion along the x-axis and the y-axis. We first regard the models for the x-axis and then for the y-axis.

4.1 Models for the temporal prediction

Before discussing the established and new motion models, we analyze the development of the velocities to obtain insights into the motion behavior of the particles. For this, we determine the mean and standard deviation of the velocities over the course of the belt. In our ground truth, we do not have the velocities of the particles at equidistant grid points along the x-axis, which we require to calculate the means. Therefore, we interpolate the velocities linearly along the x-axis. Using this interpolation, we can calculate the mean and standard deviation of the velocities over the course of the belt. In Fig. 7, we visualize the results for three different bulk materials. While we must be careful as the perceived linearity in the plot is regarding the position on the belt and not the time, we can see that there is a clear trend toward further acceleration. Proper models must take this into account.

For the models for the prediction to the separation mechanism, we start with an interpretation of the old, implicit model and then proceed with the CV model used in [15]. Afterward, we introduce a modified version of the

CV model, and then explain the CA model and two more sophisticated models. As we focus on the prediction to a specific coordinate x^{PredTo} along the x-axis at which the separation is supposed to occur, we use continuous-time formulations for all models to derive the accurate point in time t^{Pred} at which the particle passes x^{PredTo}.

Identical delay (ID) and identical velocity (IV) model
In the old, implicit model, the assumption about the motion along the transport direction is simply that the particles pass the separation mechanism after a fixed delay. Thus, we refer to the part of the old, implicit model describing the motion in transport direction as identical delay (ID) model. In this model, the predicted time $t^{\mathrm{Pred,ID}}$ is calculated from the average time that passes between the last observation of a particle and its arrival at the separation mechanism t^{Avg} and the time of the last observation of the particle t^{Last} according to

$$t^{\mathrm{Pred,ID}} = t^{\mathrm{Last}} + t^{\mathrm{Avg}} .$$

For line scan cameras, the accuracy of the determined time at which the centroid of a particle passed the camera t^{Last} may be limited by the temporal resolution of the camera. However, due to the high frame rates of line scan cameras, the temporal resolution is so high (compared with the temporal resolution of the separation mechanism) that the imprecision can usually be neglected.

The ID model is implicitly based on the assumption that the x-coordinate x^{Last} at which the particle is observed last is identical for all particles. While this holds for line scan cameras, this is generally not a valid assumption when using area scan cameras. To provide the most favorable conditions to the old, implicit model when it is used for area scan cameras, we use an interpretation of the model with less strict assumptions for the remainder of this paper. We strip the model of the assumption of an identical x-coordinate and assume that all particles have the same velocity instead. This leads to the model

$$t^{\mathrm{Pred,IV}} = t^{\mathrm{Last}} + \frac{x^{\mathrm{PredTo}} - x^{\mathrm{Last}}}{\dot{x}^{\mathrm{Avg}}} , \qquad (1)$$

which we refer to as identical velocity (IV) model. This model requires the average velocity of the particles during the prediction phase $\dot{x}^{\mathrm{Avg}}$ and is equivalent to the ID model if x^{Last} is always identical.

Constant velocity (CV) model
For tracking the particles in the tracking phase in discrete time, the constant velocity model for the x-axis is based on

the individually estimated position x_k and velocity $\dot{x}_k$ and is given by

$$x_{k+1} = x_k + \Delta t\, \dot{x}_k\,, \tag{2}$$

with Δt describing the temporal gap between time step k and $k + 1$. To bridge the prediction phase, we use the continuous-time CV model

$$x(t) = x^{\text{Last}} + (t - t^{\text{Last}})\dot{x}^{\text{Last}}\,, \tag{3}$$

in which $\dot{x}^{\text{Last}}$ is the last estimate of the velocity of the particle in the tracking phase. Due to the lack of measurements, the velocity estimate does not change during the prediction phase.

To obtain the predicted time $t^{\text{Pred,CV}}$, the remaining distance is divided by $\dot{x}^{\text{Last}}$, resulting in the formula

$$t^{\text{Pred,CV}} = t^{\text{Last}} + \frac{x^{\text{PredTo}} - x^{\text{Last}}}{\dot{x}^{\text{Last}}}\,.$$

However, as discussed in the introduction of this section, this model results in a bias when the particles accelerate further during the prediction phase, which can occur when they are still on the belt. A bias can also result from deceleration, which can occur due to air resistance when the particles are in flight.

To eliminate the bias, we define a bias correction term t^{BC} that is the median of the differences between the true times t^{GT} and the predicted times $t^{\text{Pred,CV}}$ for all particles observed in the calibration phase. Using the median provides more robustness to outliers than using the mean. In our scenario, outliers should be disregarded because beyond a certain error, the particle will not be hit and thus, the actual deviation from the true value becomes irrelevant. The formula for a CV model with bias correction (CVBC) using the correction term t^{BC} is given by

$$t^{\text{Pred,CVBC}} = t^{\text{Last}} + \frac{x^{\text{PredTo}} - x^{\text{Last}}}{\dot{x}^{\text{Last}}} + t^{\text{BC}}\,.$$

It should be noted that the correction term t^{BC} does not respect where the particles are along the x-axis at their last observation. A model in which the bias is corrected differently is explained after the constant acceleration model.

Constant acceleration (CA) model

During the tracking phase, we can use the discrete-time constant acceleration model, which includes the particle's acceleration $\ddot{x}_k$ and can be written as

$$\begin{aligned} x_{k+1} &= x_k + \Delta t\, \dot{x}_k + \frac{1}{2}(\Delta t)^2 \ddot{x}_k\,, \\ \dot{x}_{k+1} &= \dot{x}_k + \Delta t\, \ddot{x}_k\,. \end{aligned} \tag{4}$$

In a multitarget tracker based on recursive Bayesian estimation, uncertainties have to be updated. We update these according to the white-noise jerk model [18].

For the continuous-time prediction to the separation mechanism, we use the last estimates of our tracker x^{Last}, $\dot{x}^{\text{Last}}$, and $\ddot{x}^{\text{Last}}$ to obtain

$$x(t) = x^{\text{Last}} + (t - t^{\text{Last}})\dot{x}^{\text{Last}} + \frac{1}{2}(t - t^{\text{Last}})^2 \ddot{x}^{\text{Last}}\,. \tag{5}$$

To find the presumed time of arrival at the separation mechanism, we determine when $x(t) = x^{\text{PredTo}}$ holds by finding the roots of

$$x^{\text{Last}} - x^{\text{PredTo}} + (t - t^{\text{Last}})\dot{x}^{\text{Last}} + \frac{1}{2}(t - t^{\text{Last}})^2 \ddot{x}^{\text{Last}}\,. \tag{6}$$

Since this is a quadratic polynomial, the roots can be found analytically. The predicted time $t^{\text{Pred,CA}}$ is the smallest real-valued root for which $(t - t^{\text{Last}}) > 0$ s holds.

Usually, the particles' velocities do not surpass the belt velocity.[3] Therefore, we propose an adjusted version of the constant acceleration model in which the velocity can be limited to a maximum velocity $\dot{x}^{\text{MaxVel}}$ (e. g., the belt velocity). For this, we first determine t^{MaxVel}, which is the point in time after t^{Last} at which the maximum velocity is (if ever) reached. We obtain t^{MaxVel} by solving

$$\dot{x}^{\text{Last}} + \ddot{x}^{\text{Last}} t = \dot{x}^{\text{MaxVel}}$$

for t. The belt velocity can only be exceeded if $\ddot{x}^{\text{Last}} > 0$ m/s^2 holds. Further, if

$$\begin{aligned} \dot{x}^{\text{Last}}(t^{\text{Last}} - t^{\text{MaxVel}}) + \frac{1}{2}\ddot{x}^{\text{Last}}(t^{\text{Last}} - t^{\text{MaxVel}})^2 \\ \leq x^{\text{Last}} - x^{\text{PredTo}} \end{aligned}$$

holds, then the maximum velocity is never surpassed until x^{PredTo}, and thus, the prediction of this model is identical to the prediction of the CA model. If $\dot{x}^{\text{MaxVel}}$ is reached before the particle passes x^{PredTo}, we use the CA model until t^{MaxVel} and use the CV model with a velocity of $\dot{x}^{\text{MaxVel}}$ for the remaining distance. This results in the formula

$$\begin{aligned} t^{\text{Pred,CALV}} = t^{\text{MaxVel}} + \Big(x^{\text{PredTo}} - x^{\text{Last}} \\ - \dot{x}^{\text{Last}}(t^{\text{MaxVel}} - t^{\text{Last}}) - \frac{1}{2}\ddot{x}^{\text{Last}}(t^{\text{MaxVel}} - t^{\text{Last}})^2 \Big)/\dot{x}^{\text{Belt}} \end{aligned}$$

for calculating the predicted time for the constant acceleration model with limited velocity (CALV).

---

3 An exception is, e. g., if the particles are applied to the belt at a higher velocity than the belt velocity.

Identical acceleration (IA) model

While the models based on the old, implicit model and the CVBC model rely on parameters that need to be determined in a calibration phase, the CV and CA models are free from such extra information and solely use information that can be obtained while the individual particles are in the tracking phase (only a maximum velocity is needed for the CALV model). We now present a sophisticated model that uses both particle-specific information and additional parameters that can be obtained in a calibration phase. In the model that we call the identical acceleration (IA) model, we assume that the particles accelerate at a constant rate as in the CA model. However, instead of using an individually estimated acceleration for each particle, we assume that all particles accelerate similarly during the prediction phase. To obtain a suitable acceleration, we determine which accelerations would have resulted in optimal predictions for the particles observed during the calibration phase. For each of these particles, we have a reference value t^{Ref} that is approximately equal to the true time at which the particle arrived at x^{PredTo}. For each particle, we use the corresponding reference value to determine $\ddot{x}^{\text{Opt}}$ that fulfills

$$x^{\text{PredTo}} = x^{\text{Last}} + (t^{\text{Ref}} - t^{\text{Last}})\dot{x}^{\text{Last}} + \frac{1}{2}(t^{\text{Ref}} - t^{\text{Last}})^2 \ddot{x}^{\text{Opt}}.$$

Then, we define $\ddot{x}^{\text{Avg}}$ to be the median of all $\ddot{x}^{\text{Opt}}$. To perform a prediction, we replace the estimated velocity of the particle with $\ddot{x}^{\text{Avg}}$ in the formula for the CA model to obtain

$$x(t) = x^{\text{Last}} + (t - t^{\text{Last}})\dot{x}^{\text{Last}} + \frac{1}{2}(t - t^{\text{Last}})^2 \ddot{x}^{\text{Avg}} .$$

In essence, $\ddot{x}^{\text{Avg}}$ summarizes all accelerating effects during the prediction phase into one acceleration that consistently affects the particle during the entire prediction phase. Such effects can be accelerations while the particles are on the belt and decelerations while the particles are in the flight phase. The term $\ddot{x}^{\text{Avg}}$ can also take into account that particles may accelerate temporarily and then slow down, e. g., because they reach the end of the belt. Because the IA model includes particle-specific velocity estimates, it does not treat all particles equally as the old, implicit model.

4.2 Models for predicting the position at the separation mechanism

Again, we start by analyzing the velocities over the course of the belt. Due to the symmetry of the scenario, the expected velocity of all particles orthogonal to the transport direction is (given a perfect calibration) zero. Therefore, we regard the velocities of individual particles for further insights. In Fig. 8, we depict multiple particles' velocities orthogonal to the transport direction for three different bulk materials. We can observe a general trend toward deceleration (more precisely, reduction in the absolute value of the velocity) as the particles move along the belt. For cuboids, a significant and almost linear decrease can be observed. For spheres, the decelerating effect is less pronounced. For cylinders, there is also a significant number of particles that accelerate. For spheres and cuboids, we believe that increases in the velocity along the y-axis after the particles were applied to the belt are mainly caused by collisions, which are hard to model without detailed knowledge about the particles. For cylinders, rolling motions may also cause accelerations if changes in the orientation around the z-axis (i. e., yaw axis) occur.

We describe the established and new models, starting with an interpretation of the old, implicit model. Then, we regard the CV and CA models. In our explanations, we assume that t^{Pred} was already determined (e. g., according to one of the models presented in the previous subsection). For brevity, we write

$$t^{\text{Diff}} = t^{\text{Pred}} - t^{\text{Last}} .$$

Straight movement model

In the old, implicit model, it is assumed that there is no movement orthogonal to the transport direction. The choice as to which valve to activate only depends on the location of the particle along the y-axis at the time of the observation. Visually speaking, the point at which the particle is detected is projected orthogonally onto the line along which the array of nozzles is aligned. The prediction model is thus simply

$$y^{\text{Pred,Straight}} = y^{\text{Last}} .$$

Constant velocity (CV) model and constant acceleration (CA) model

For the CV and CA models, the discrete-time versions used during the tracking phase are the analogues to (2) and (4) for the y-axis. For the prediction to the separation, we first regard the CV model. For this model, we use the temporal evolution of the y-axis position in continuous time, which is analogous to the evolution along the x-axis given in (3), and insert the known time difference t^{Diff} to obtain

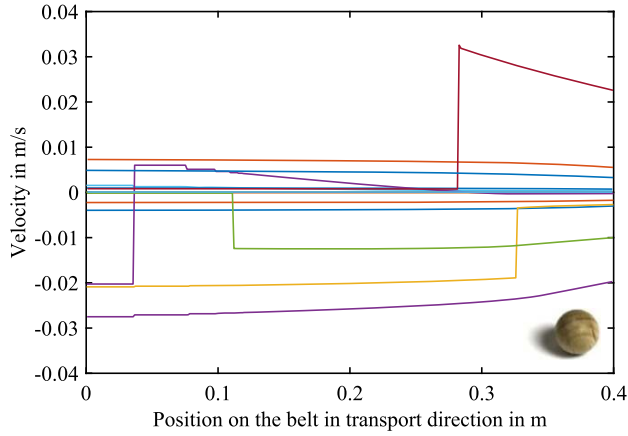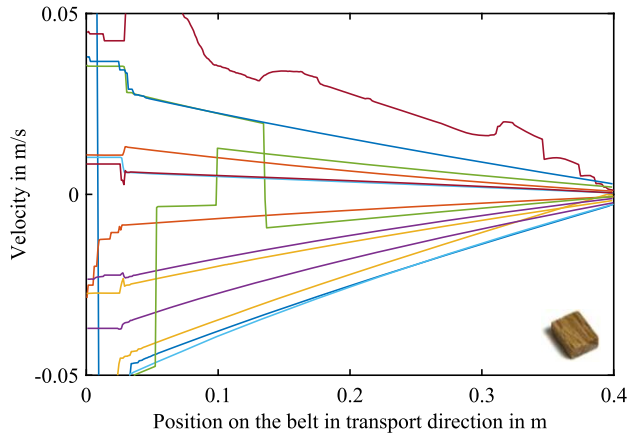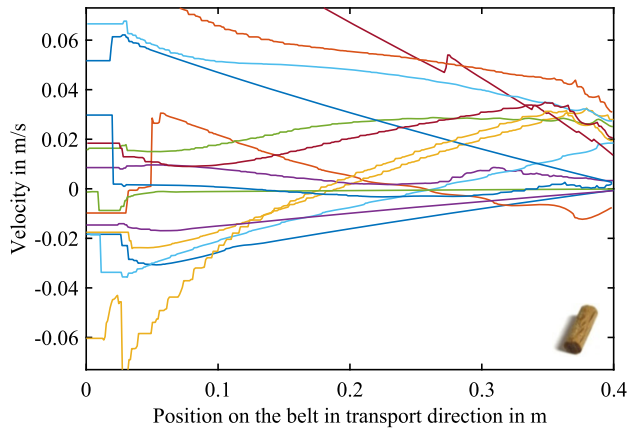$$y^{\text{Pred,CV}} = y^{\text{Last}} + t^{\text{Diff}} \dot{y}^{\text{Last}} .$$

(a) Examples for velocities along the y-axis for spheres.

(b) Examples for velocities along the y-axis for cuboids.

(c) Examples for velocities along the y-axis for cylinders.

Figure 8: Velocities along the y-axis over the course of the belt for the three bulk materials considered. To ensure the clarity of the plots, the velocities were plotted for only 15 particles.

We proceed similarly for the CA model. The evolution of the position along the y-axis is analogous to that along the x-axis described by (5). Inserting the predicted time into the formula, we obtain

$$y^{\text{Pred,CA}} = y^{\text{Last}} + t^{\text{Diff}} \dot{y}^{\text{Last}} + \frac{1}{2}(t^{\text{Diff}})^2 \ddot{y}^{\text{Last}} \qquad (7)$$

as the formula for the prediction of the CA model.

Scenario-specific models

In our first scenario-specific model, we integrate the knowledge that changes in the velocity of the particles are mainly caused by the friction between the particles and the belt. Without considering additional effects, the particles are expected to come to a halt relative to the belt. Thus, we expect a decrease in the absolute value of the velocity along the y-axis and do not expect a reversal of the direction in which the particles move. To integrate this knowledge in the model, we first determine when the currently considered particle will come to halt, given the assumption of a constant acceleration. This point in time, which we call $t^{\text{SignChange}}$, can be calculated according to

$$t^{\text{SignChange}} = t^{\text{Last}} + \frac{-\dot{y}^{\text{Last}}}{\ddot{y}^{\text{Last}}} \ .$$

If $t^{\text{SignChange}} < t^{\text{Last}}$ or $t^{\text{SignChange}} \geq t^{\text{Pred}}$, the prediction is identical to that of the CA model. Otherwise, we assume the particle stays stationary along the y-axis from $t^{\text{SignChange}}$ on. Thus, we obtain the formula

$$y^{\text{Pred,CADSC}} = y^{\text{Last}} + (t^{\text{SignChange}} - t^{\text{Last}}) \dot{y}^{\text{Last}}$$
$$+ \frac{1}{2}(t^{\text{SignChange}} - t^{\text{Last}})^2 \ddot{y}^{\text{Last}}$$

for predicting the position along the y-axis when using a constant acceleration model disallowing sign changes (CADSC) in the velocity orthogonal to the transport direction.

For the next model, we consider additional information that can be derived in a calibration phase. We cannot use the IA model for the y-axis since the average acceleration would be close to zero due to the symmetry of the scenario. In the new model, which we refer to as the ratio-based model, we determine a suitable acceleration that respects each individual particle's velocity (including its sign). For all particles observed during the calibration phase, we determine the ratio between the velocity of the particle when it reaches the prediction target and the velocity at the beginning of the prediction phase $\dot{y}^{\text{Last}}$. For all particles observed in the calibration phase, we calculate the quotient of these two velocities (omitting all terms

that involve a division by zero). Then, we take the median all quotients and call it r.

We assume that for all particles observed in the future, the remaining velocity at the end of the prediction phase will be approximately $r\dot{y}^{\text{Last}}$. This means the absolute change in the velocity that occurs during the prediction phase is assumed to be

$$\dot{y}^{\text{Change}} = -(1 - r)\,\dot{y}^{\text{Last}} .$$

We further assume that the acceleration along the y-axis is constant during the prediction phase. This leads to the formula

$$\ddot{y}^{\text{Ratio}} = \frac{\dot{y}^{\text{Change}}}{t^{\text{Diff}}} .$$

Because $\dot{y}^{\text{Last}}$ is particle specific, $\ddot{y}^{\text{Ratio}}$ also generally differs for different particles. To determine the prediction, we use $\ddot{y}^{\text{Ratio}}$ as the acceleration in the formula for the CA model and obtain the formula

$$y^{\text{Pred,Ratio}} = y^{\text{Last}} + t^{\text{Diff}}\dot{y}^{\text{Last}} + \frac{1}{2}(t^{\text{Diff}})^2\ddot{y}^{\text{Ratio}} .$$

5 Evaluation

In our evaluation, we put the models for both axes to a test. To be in line with real-world challenges, we evaluate the precision of the prediction regarding the time and place at which the particles reach the separation mechanism. As in the previous sections, we assume the separation occurs immediately after the particles leave the belt. The tracking phase starts at the beginning of the belt and ends with the beginning of the prediction phase, which starts 15 cm before the end of the belt. As in the development of the models, we use the ground truth data downsampled to 1000 Hz. Only the data obtained during the tracking phase are used to generate the predictions to the separation mechanism. To obtain reference values to compare the prediction with, we proceed as illustrated in Fig. 5. While these reference values are approximations of the ground truth values, they are highly accurate compared with the predictions that are generated 15 cm before the end of the belt. The simulation data contains approximately 115 positions of each particle during the prediction phase, but we only use the last observation before reaching the separation mechanism (which is not enabled for our evaluation) and the first observation thereafter to obtain the reference values (see Fig. 5).

Using our new models, we aim to outperform the old, implicit model as employed by optical belt sorters based on line scan cameras. Therefore, we determine the actual median of the velocities of all particles for the IV model to use this model under the most favorable conditions. For our new models, we avoid unrealistically favorable conditions and use at most 1% of all particles available (37 to 44, depending on the data set) to determine the required parameters. We explain how the temporal and spatial deviations were calculated in the first subsection. Afterward, we present the evaluation results regarding the temporal component (along the x-axis) and the spatial component (along the y-axis) in the second and third subsection.

5.1 Determining the temporal and spatial deviations

For each combination of models, we first determine the temporal component of the prediction t^{Pred}. Afterward, we calculate the spatial prediction y^{Pred} based on t^{Pred}, as laid out in Sec. 4.2. Unlike in [15], we never use the ground truth velocity at the end of the tracking phase provided by the DEM simulation. In [15], the ground truth velocities were only used to assess the maximum performance of the CV model, but as expected, the results were very close to those obtained when approximating the velocities based on the position data. In our current evaluation, we only use information that would be available in real-world tracking applications and derive all velocities and accelerations from the position measurements. To determine the velocities and accelerations, only the last few observations are required because the simulation data are free from stochastic noise.

We calculated the deviations by subtracting the predictions from the reference values. The temporal and spatial deviations are visualized using box plots. The red line in the middle of each box shows the median and the box ranges from the 25th to the 75th percentile. The whiskers on top of and below the boxes extend to the value that deviates at most $\pm 2.7\sigma$ from the median, which corresponds to a coverage of up to approximately 99.3% if the data are normally distributed. All values beyond the whiskers are considered outliers. As visualizing all outliers would require using different axis limits and would decrease the clarity of the plots, we do not show any outliers.

5.2 Temporal deviations

For the temporal deviations, we compare the results of the identical velocity model (IV), the constant velocity

(a) Temporal deviations for the spheres data set.

(b) Temporal deviations for the cuboids data set.

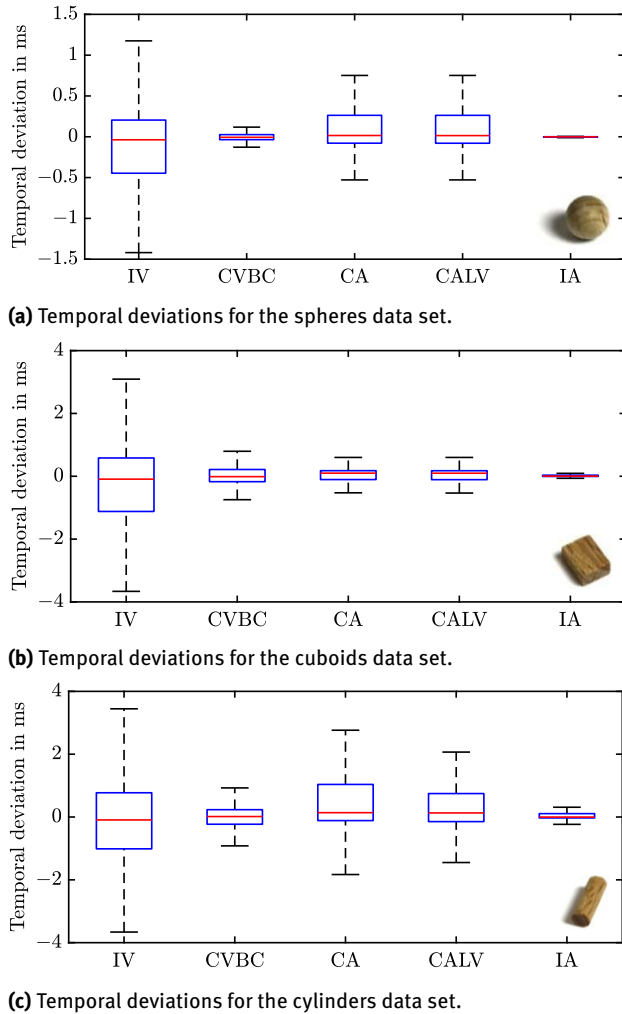**(c)** Temporal deviations for the cylinders data set.

Figure 9: Evaluation results for all data sets regarding the temporal component of the error. A positive number means that the particle arrived earlier than anticipated whereas a negative number indicates that it arrived later than expected. Adapted version of a plot from [16].

model with bias correction (CVBC), the constant acceleration model (CA), the constant acceleration model with limited velocity (CALV), and the identical acceleration model (IA). The evaluation results are shown in Fig. 9. Due to large biases that would necessitate different axis limits for a proper visualization, we omit the CV model without bias correction. Results for this model are provided in [16, Ch. 4].

Out of the models considered, the IV model results in the highest deviations in all data sets. The assumption of an identical velocity for all particles, as used in the old, implicit model, is thus rather inaccurate. While not shown in the plots, the CV model without bias correction is the worst model overall for the temporal predictions in all scenarios due to the large biases. However, even by merely using the

simple bias correction, the CV model can be turned into one of the best models. The CA model performed worse than the CVBC model except in the cuboids data set. However, the CA model performs better than the IV model and does not suffer from large biases. Thus, this model may be suitable for scenarios in which it is clear that the particles accelerate further but it is infeasible to obtain the additional parameter for the IA model. Using the CALV model does not yield large improvements, which is explained by the fact that only few particles are predicted to exceed the belt velocity when using a CA model. The best model in all three scenarios is the IA model. This shows that although assuming an identical velocity for all particles yields insufficient prediction accuracy, assuming an identical acceleration for all particles is better than assuming that the individually estimated accelerations of the particles at the end of the tracking phase are maintained.
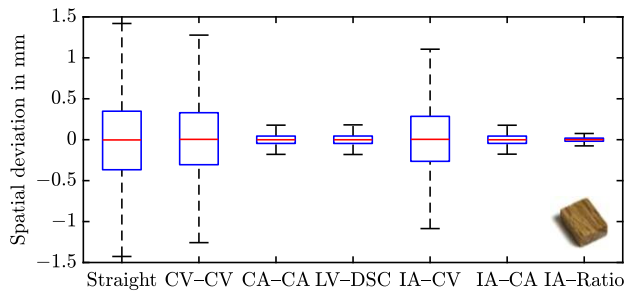
5.3 Spatial deviations

As previously mentioned, the models for the motion along the y-axis can be combined with different models for the x-axis. We evaluate the straight prediction model (which is independent of the model for the x-axis), the constant velocity model along both axes (CV–CV), the constant acceleration model along both axes (CA–CA), and the constant acceleration model with limited velocity along the x-axis in combination with the constant acceleration model without sign change for the y-axis (CALV–CADSC, or LV–DSC for brevity). Further, due to its highly accurate temporal predictions, we combine the IA model along the x-axis with three different models for the y-axis, namely the CV and CA models (IA–CV and IA–CA), and the ratio-based model (IA-Ratio).

The results are given in Fig. 10. It can be seen that the straight prediction model performs the worst in all scenarios. This shows that accounting for motion orthogonal to the transport direction, which was an important motivation for predictive tracking, is key to obtaining highly accurate predictions. Even using the CV model leads to significant improvements. Previous research [8] also documents the superiority of the CV model over the straight prediction model for real data recorded on an industrial-scale optical belt sorter. The CA model is superior to the CV model in two of the three scenarios. The modification disallowing a sign change does not yield an improvement. In the cylinders data set, sign changes, which lead to errors in the CADSC model, do occur (see Fig. 8c). The lack of improvement in the other scenarios suggests that it may not be necessary to use this modified version of the CA model.
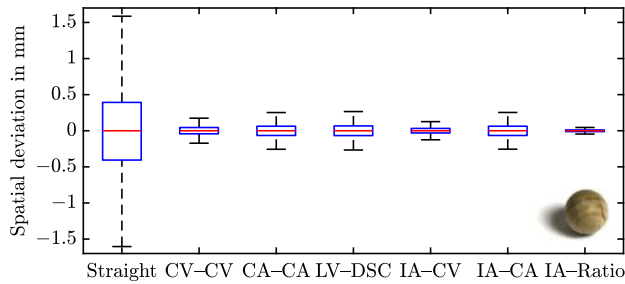
(a) Spatial deviations for the spheres data set.

(b) Spatial deviations for the cuboids data set.
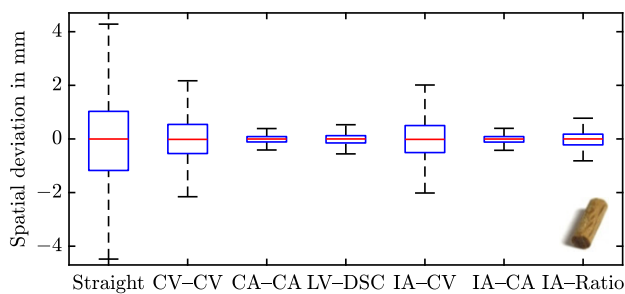
(c) Spatial deviations for the cylinders data set.

Figure 10: Evaluation results for all data sets regarding the spatial component of the error.

Combining the IA model, which is the best model for predicting the motion along the transport direction in the considered scenarios, with the CV and CA models (IA–CV and IA–CA) does not result in large improvements over the combinations CV–CV and CA–CA. The combination of the IA model with the ratio-based model along the *y*-axis performs is superior to all other combinations for the spheres and cuboids data sets. However, like the CADSC model, the ratio-based model does not allow for reversals of the direction of the motion along the *y*-axis, which is a possible cause for the lower performance in the cylinders data set.

6 Conclusion

In this paper, we analyzed the behavior of bulk material particles in an optical belt sorter to derive suitable mod-

els for the predictive tracking approach. Assuming that all particles have an identical velocity along the transport direction and a velocity of zero orthogonal to the transport direction, as done in line scan camera-based optical belt sorters, may result in large errors even if accurate information on the average velocity of the particles is available. One must also be cautious when using a constant velocity model since accelerations and decelerations along the transport direction during the prediction phase may cause a bias in the temporal predictions. Accelerations may occur for short belts and large differences between the initial velocities of the particles and the belt velocity and decelerations can arise from the decelerating effect of air resistance when the overlap between the prediction phase and the flight phase is not negligible. Using the constant acceleration model is a good option if the particles are still accelerating and no further knowledge is available. By observing only a few particles at the end of the prediction phase (e. g., in a calibration phase) and assuming that all particles accelerate similarly, we can provide a very good model for the motion along the transport direction. Similarly, for the motion orthogonal to the transport direction, integrating knowledge about the average remaining velocity at the separation mechanism can lead to significant improvements. However, the superiority of the predictions over those of a constant acceleration model is not as pronounced as in the case of the model for the motion along the transport direction.

All in all, the choice of the motion model has a large impact on the accuracy of the predictions. Using suitable models, the hardware expenses to decrease motion orthogonal to the transport direction can be reduced. Furthermore, particles can be targeted accurately even if they are still accelerating and differ in their velocities at the end of the tracking phase. In future work, more sophisticated models could be derived, e. g., using all observations of some particles in the prediction phase or by integrating the orientations of the particles in the motion model. Data-driven machine learning approaches could also be considered for creating new particle-specific motion models. Moreover, we plan to evaluate the models using real image data to verify that the new models are also superior in real-world applications. Especially evaluating the sorting quality including the actual separation step and its imprecisions will allow us to not only evaluate the models but also to draw further conclusions such as whether using a faster belt loaded with a low number of particles is to be preferred over a slow belt loaded with a high number of particles.

References

1. J. Duran, *Sands, Powders, and Grains: An Introduction to the Physics of Granular Materials*. Springer-Verlag, 2000.
2. Y.-S. Chen, S.-S. Hsiau, H.-Y. Lee, Y.-P. Chyou and C.-J. Hsu, "Size Separation of Particulates in a Trommel Screen System," *Chemical Engineering and Processing: Process Intensification*, vol. 49, no. 11, 2010.
3. J. Oberteuffer, "Magnetic Separation: A Review of Principles, Devices, and Applications," *IEEE Transactions on Magnetics*, vol. 10, no. 2, pp. 223–238, Jun. 1974.
4. F. Brandt and R. Haus, "New Concepts for Lithium Minerals Processing," *Minerals Engineering*, vol. 23, no. 8, pp. 659–661, 2010.
5. R. Mattone, G. Campagiorni and F. Galati, "Sorting of Items on a Moving Conveyor Belt. Part 1: A Technique for Detecting and Classifying Objects," *Robotics and Computer-Integrated Manufacturing*, vol. 16, no. 2, pp. 73–80, 2000.
6. M. Graves and B. Batchelor, *Machine Vision for the Inspection of Natural Products*. Springer Science & Business Media, 2003.
7. H. U. R. Kattentidt, T. P. R. De Jong and W. L. Dalmijn, "Multi-Sensor Identification and Sorting of Bulk Solids," *Control Engineering Practice*, vol. 11, no. 1, 2003.
8. F. Pfaff, M. Baum, B. Noack, U. D. Hanebeck, R. Gruna, T. Längle and J. Beyerer, "TrackSort: Predictive Tracking for Sorting Uncooperative Bulk Materials," in *Proceedings of the 2015 IEEE International Conference on Multisensor Fusion and Integration for Intelligent Systems (MFI 2015)*, San Diego, California, USA, Sep. 2015.
9. G. Maier, F. Pfaff, F. Becker, C. Pieper, R. Gruna, B. Noack, H. Kruggel-Emden, T. Längle, U. D. Hanebeck, S. Wirtz, V. Scherer and J. Beyerer, "Motion-Based Material Characterization in Sensor-Based Sorting," *tm – Technisches Messen, De Gruyter*, Oct. 2017.
10. S. Blackman and R. Popoli, *Design and Analysis of Modern Tracking Systems*, 1999.
11. R. P. S. Mahler, *Statistical Multisource-Multitarget Information Fusion*. Artech House, Inc., 2007.
12. G. Maier, F. Pfaff, C. Pieper, R. Gruna, B. Noack, H. Kruggel-Emden, T. Längle, U. D. Hanebeck, S. Wirtz, V. Scherer and J. Beyerer, "Fast Multitarget Tracking via Strategy Switching for Sensor-Based Sorting," in *Proceedings of the 2016 IEEE International Conference on Multisensor Fusion and Integration for Intelligent Systems (MFI 2016)*, Baden-Baden, Germany, Sep. 2016.
13. G. Maier, F. Pfaff, M. Wagner, C. Pieper, R. Gruna, B. Noack, H. Kruggel-Emden, T. Längle, U. D. Hanebeck, S. Wirtz, V. Scherer and J. Beyerer, "Real-Time Multitarget Tracking for Sensor-Based Sorting," *Journal of Real-Time Image Processing*, Nov. 2017.
14. C. Pieper, G. Maier, F. Pfaff, H. Kruggel-Emden, S. Wirtz, R. Gruna, B. Noack, V. Scherer, T. Längle, J. Beyerer and U. D. Hanebeck, "Numerical Modeling of an Automated Optical Belt Sorter Using the Discrete Element Method," *Powder Technology*, Jul. 2016.
15. F. Pfaff, C. Pieper, G. Maier, B. Noack, H. Kruggel-Emden, R. Gruna, U. D. Hanebeck, S. Wirtz, V. Scherer, T. Längle and J. Beyerer, "Simulation-Based Evaluation of Predictive Tracking for Sorting Bulk Materials," in *Proceedings of the 2016 IEEE International Conference on Multisensor Fusion and Integration for Intelligent Systems (MFI 2016)*, Baden-Baden, Germany, Sep. 2016.
16. F. Pfaff, "Multitarget Tracking Using Orientation Estimation for Optical Belt Sorting," Ph.D. dissertation, Karlsruhe Institute of Technology, 2018.
17. F. Pfaff, G. Maier, M. Aristov, B. Noack, R. Gruna, U. D. Hanebeck, T. Längle, J. Beyerer, C. Pieper, H. Kruggel-Emden, S. Wirtz and V. Scherer, "Real-Time Motion Prediction Using the Chromatic Offset of Line Scan Cameras," *at – Automatisierungstechnik, De Gruyter*, Jun. 2017.
18. X. R. Li and V. P. Jilkov, "Survey of Maneuvering Target Tracking. Part I. Dynamic Models," *IEEE Transactions on Aerospace and Electronic Systems*, vol. 39, no. 4, pp. 1333–1364, 2003.
19. F. Pfaff, C. Pieper, G. Maier, B. Noack, H. Kruggel-Emden, R. Gruna, U. D. Hanebeck, S. Wirtz, V. Scherer, T. Längle and J. Beyerer, "Improving Optical Sorting of Bulk Materials Using Sophisticated Motion Models," *tm – Technisches Messen, De Gruyter*, vol. 83, no. 2, pp. 77–84, Feb. 2016.
20. P. A. Cundall and O. D. L. Strack, "A Discrete Numerical Model for Granular Assemblies," *Géotechnique*, vol. 29, no. 1, pp. 47–65, 1979.
21. C. Pieper, F. Pfaff, G. Maier, H. Kruggel-Emden, S. Wirtz, B. Noack, R. Gruna, V. Scherer, U. D. Hanebeck, T. Längle and J. Beyerer, "Numerical Modelling of an Optical Belt Sorter Using a DEM–CFD Approach Coupled with a Particle Tracking Algorithm and Comparison with Experiments," *Powder Technology*, Dec. 2018.
22. R. S. Fitzpatrick, H. J. Glass and R. D. Pascoe, "CFD–DEM Modelling of Particle Ejection by a Sensor-Based Automated Sorter," *Minerals Engineering*, vol. 79, pp. 176–184, 2015.
23. C. Pieper, G. Maier, F. Pfaff, H. Kruggel-Emden, R. Gruna, B. Noack, S. Wirtz, V. Scherer, T. Längle, U. D. Hanebeck and J. Beyerer, "Numerical Modelling of the Separation of Complex Shaped Particles in an Optical Belt Sorter Using a DEM–CFD Approach and Comparison with Experiments," in *Proceedings of the 5th International Conference on Particle-Based Methods (PARTICLES 2017)*, Hannover, Germany, Sep. 2017.
24. D. Höhner, S. Wirtz and V. Scherer, "Experimental and Numerical Investigation on the Influence of Particle Shape and Shape Approximation on Hopper Discharge Using the Discrete Element Method," *Powder Technology*, vol. 235, pp. 614–627, 2013.

Bionotes

Florian Pfaff
Intelligent Sensor-Actuator-Systems
Laboratory (ISAS), Karlsruhe Institute of
Technology (KIT), Karlsruhe, Germany
florian.pfaff@kit.edu

Florian Pfaff is a postdoctoral researcher at the Intelligent Sensor-Actuator-Systems Laboratory at the Karlsruhe Institute of Technology. He obtained his diploma in 2013 and his Ph.D. in 2018, both with the highest distinction. His research interests include a variety of estimation problems such as filtering on nonlinear manifolds, multitarget tracking, and estimation in the presence of both stochastic and non-stochastic uncertainties.

Christoph Pieper
Department of Energy Plant Technology
(LEAT), Ruhr-Universität Bochum (RUB),
Bochum, Germany

Christoph Pieper is a research assistant at the Department of Energy Plant Technology at the Ruhr University Bochum. His research interests include numerical simulation of fluidized particle systems with the Discrete Element Method (DEM) and Computational Fluid Dynamics (CFD).

Georg Maier
Fraunhofer IOSB, Fraunhofer Institute of
Optronics, System Technologies and Image
Exploitation, Karlsruhe, Germany

Georg Maier is with the Fraunhofer Institute of Optronics, System Technologies and Image Exploitation IOSB, Karlsruhe, Germany. His research interests include different aspects of image processing, in particular algorithmic aspects, with a focus on real-time capabilities.

Benjamin Noack
Intelligent Sensor-Actuator-Systems
Laboratory (ISAS), Karlsruhe Institute of
Technology (KIT), Karlsruhe, Germany

Benjamin Noack is a senior researcher at the Intelligent Sensor-Actuator-Systems Laboratory at the Karlsruhe Institute of Technology (KIT), Germany. His research interests are in the areas of multi-sensor data fusion, distributed and decentralized Kalman filtering, combined stochastic and set-membership approaches to state estimation, and event-based systems.

Robin Gruna
Fraunhofer IOSB, Fraunhofer Institute of
Optronics, System Technologies and Image
Exploitation, Karlsruhe, Germany

Robin Gruna is research group manager at the Fraunhofer Institute of Optronics, System Technologies and Image Exploitation IOSB in Karlsruhe, Germany. His research interests include spectral imaging, machine learning, and computational imaging.

Harald Kruggel-Emden
Mechanical Process Engineering and Solids
Processing (MVTA), Technical University
Berlin, Berlin, Germany

Harald Kruggel-Emden is professor and head of the department of Mechanical Process Engineering and Solids Processing at the Technical University of Berlin. His research interests include Discrete Element Modelling with coupled fluid flow, material preparation and drying technology, bulk solids handling, and chemical looping combustion.

Uwe D. Hanebeck
Intelligent Sensor-Actuator-Systems
Laboratory (ISAS), Karlsruhe Institute of
Technology (KIT), Karlsruhe, Germany

Uwe D. Hanebeck is a chaired professor of Computer Science at the
Karlsruhe Institute of Technology (KIT) in Germany and director of
the Intelligent Sensor-Actuator-Systems Laboratory (ISAS). He ob-
tained his Ph.D. degree in 1997 and his habilitation degree in 2003,
both in Electrical Engineering from the Technical University in Mu-
nich, Germany. His research interests are in the areas of information
fusion, nonlinear state estimation, stochastic modeling, system
identification, and control with a strong emphasis on theory-driven
approaches based on stochastic system theory and uncertainty
models. He is author and coauthor of more than 500 publications in
various high-ranking journals and conferences and an IEEE Fellow.

Siegmar Wirtz
Department of Energy Plant Technology
(LEAT), Ruhr-Universität Bochum (RUB),
Bochum, Germany

Siegmar Wirtz is the deputy head of the Department of Energy Plant
Technology at the Ruhr University Bochum. His research interests
include numerical simulation of reactive gas–solid flows, extension
of commercial CFD codes, and Discrete Element Modelling with
coupled fluid flow.

Viktor Scherer
Department of Energy Plant Technology
(LEAT), Ruhr-Universität Bochum (RUB),
Bochum, Germany

Viktor Scherer is the head of the Department of Energy Plant Tech-
nology at the Ruhr University Bochum. His research interests in-
clude energetic conversion of fossil fuels and biomass as well as
related industrial applications and experimental and theoretical
investigation of energy and high temperature processes.

Thomas Längle
Fraunhofer IOSB, Fraunhofer Institute of
Optronics, System Technologies and Image
Exploitation, Karlsruhe, Germany

Thomas Längle is adjunct professor at the Karlsruhe Institute of
Technology (KIT), Karlsruhe, and the head of the business unit "Vi-
sion Based Inspection Systems" (SPR) at the Fraunhofer IOSB in
Karlsruhe, Germany. His research interests include different as-
pects of image processing and real-time algorithms for inspection
systems.

Jürgen Beyerer
Fraunhofer IOSB, Fraunhofer Institute of
Optronics, System Technologies and Image
Exploitation, Karlsruhe, Germany

Jürgen Beyerer has been a full professor for informatics at the Insti-
tute for Anthropomatics and Robotics at the Karlsruhe Institute of
Technology (KIT) since March 2004 and director of the Fraunhofer
Institute of Optronics, System Technologies and Image Exploita-
tion (IOSB) in Ettlingen, Karlsruhe, Ilmenau, Lemgo, Görlitz. He
is Spokesman of the Fraunhofer Group for Defense and Security
VVS and he is member of acatech, National Academy of Science
and Engineering. Furthermore, he is Head of team 7 of the platform
"Lernende Systeme" and Spokesman of the Competence Center
Robotic Systems for Decontamination in Hazardous Environments
(ROBDEKON). Research interests include automated visual inspec-
tion, signal and image processing, pattern recognition, metrology,
information theory, machine learning, system theory security, au-
tonomous systems, and automation.